Available online at www.sciencedirect.com
ScienceDirect
Catalysis Today 126 (2007) 328–337
CATALYSIS TODAY
www.elsevier.com/locate/cattod

Toluene removal by a DBD-type plasma combined with metal oxides catalysts supported by nickel foam

Yu-fang Guo [a,1], Dai-qi Ye [a,*], Ke-fu Chen [b], Jian-cong He [a]

[a] College of Environmental Science and Engineering, South China University of Technology, Guangzhou 510640, PR China
[b] College of Resource Science and Paper-making Engineering, South China University of Technology, Guangzhou 510640, PR China

Available online 12 July 2007

Abstract

The performance on toluene removal in a dielectric barrier discharge (DBD) type plasma system under different background gases, including N_2, Ar, N_2/Ar, and N_2/O_2 was studied at room temperature and atmospheric pressure. For comparison, another laboratory-scale plasma-catalysis system was set up and four kinds of metal oxides, i.e., copper oxide, iron oxide, cobalt oxide, and manganese oxide supported on alumina/nickel foam (NF), were used as catalysts. The reaction mechanism and dynamics analysis on toluene removal were suggested. In addition, the characterization of the catalysts was performed by BET, XRD, SEM, FT-IR, and EDS. It has been found that adding argon in the background gas could improve the toluene removal efficiency significantly in the plasma system. Combining plasma with catalyst in situ could improve the toluene removal efficiency, increase the carbon dioxide selectivity and suppress byproducts formation. In addition, manganese oxide/alumina/NF was confirmed as the most effective catalyst for toluene removal. The XRD and SEM results showed that the proportion of metal oxide increased while aluminate decreased after plasma application. The granularity of the grain on the catalyst surface became smaller and the distribution became more uniform after discharge. The results of FT-IR and EDS suggested that some organic compounds deposited on the catalysts after plasma reaction.
© 2007 Elsevier B.V. All rights reserved.

Keywords: Dielectric barrier discharge; Metal oxides; VOCs; Catalyst

1. Introduction

Emissions of VOCs into atmosphere are detrimental to both human health and the global environment. The conventional means for VOCs abatement include liquid absord, activated carbon adsorption, incineration, and catalytic oxidation. But each has been restricted for its drawbacks. For example, liquid absord and activated carbon adsorption in turn have undesirable byproducts, while incineration and catalytic oxidation require high cost and energy consumption. Therefore, plasma has great industrial potential for its relatively low power consumption and high removal efficiency. In recent years, non-thermal plasma (NTP) technology has been applied to the decomposition of VOCs [1–8]. However, NTP alone has many disadvantages, such as low energy efficiencies, poor selectivity to carbon dioxide, and byproduct formation. A new attempt to overcome these limitations is the combination of the NTP method with catalysis [9–12]. By adding a catalyst to a plasma reactor, it seems possible to avoid some drawbacks of both thermal catalysis (high energy consumption) and plasma alone (ozone formation) and to improve the efficiency of the process [11]. The commercial catalysts for oxidizing VOCs can be classified into three categories: (1) supported noble metals [13,14]; (2) metal oxides or supported metals [15–17]; and (3) mixtures of noble metals and metal oxides [18]. In general, noble metal catalysts have greater activity than other metal catalysts, but their manufacturing cost is high.

In the present paper, the toluene removal performance in a plasma system under different background gases, including N_2, Ar, N_2/Ar, and N_2/O_2, was studied. For comparison, another laboratory-scale plasma-catalysis system was built up for toluene decomposition and four kinds of metal oxides, i.e., copper oxide, iron oxide, cobalt oxide, and manganese oxide supported on Al_2O_3/NF, were used as catalysts. The catalysts were placed in the discharge area of a wire-plate dielectric barrier discharge reactor. The combination effect of plasma and

* Corresponding author. Tel.: +86 20 87111279; fax: +86 20 87111279.
E-mail address: cedqye@scut.edu.cn (D.-q. Ye).
[1] Present address: College of Environmental Science and Engineering, Guangzhou University, Guangzhou 510006, PR China.

0920-5861/$ – see front matter © 2007 Elsevier B.V. All rights reserved.
doi:10.1016/j.cattod.2007.06.025

catalyst as well as the toluene removal efficiency, ozone concentration and the carbon dioxide selectivity for different catalysts was compared. The reaction mechanism and dynamics analysis on toluene removal were suggested. In addition, the characterization of the catalysts was performed by BET, XRD, SEM, FT-IR, and EDS.

2. Experimental

2.1. Experimental set up

Background gases of N_2 (>99.999%), O_2 (>99.99%), or Ar (>99.99%) from gas cylinders were generated then a set of mass flow controllers was used to regulate the flow rates. Gaseous toluene was regulated by passing part of the nitrogen gas stream through pure toluene liquid (>99.5%) kept in a water bath ($T = 25 \pm 1$ °C). High voltage power was supplied by a booster (0–250 V) cooperated with a high voltage ac transformer (50 Hz, 30 kV, root mean square voltage) in series. A digital power meter (YF9901, China) was connected to the variable voltage transformer to measure the input power. The discharge power (the power deposited to the reactor) was calculated from the applied voltage and the reactor current. The applied voltage was measured by a high-voltage probe (61010, Germany). The input power included the discharge power and the power consumption of the transformer and the circuit. In this experiment, the discharge power was proportional to the input power by a factor of 0.5–0.63 in the DBD–catalyst system and by a factor of approximately 0.35 in the DBD system.

Gas samples were obtained from the effluent by an auto-sampler and were analyzed on-line. Toluene and the reaction products were analyzed by a gas chromatograph (GC-900A, China) equipped with two hydrogen flame ionization detectors. One was for organic compounds (such as methane, benzene, and toluene) detection and used a 50 m SE-30 capillary column heated at 80 °C and the other, equipped with a methanizer, was for carbon monoxide and carbon dioxide analysis and used a 2 m carbon molecular sieve stainless steel column heated at 65 °C. The ozone concentration was monitored by an ozone analyzer (DCS-1, China). The experiment was carried out at room temperature and atmospheric pressure.

2.2. Reactor

The wire-plate DBD reactor with catalyst in situ used here is similar to that reported previously [19,20]. A superimposed wire-plate DBD reactor was used in the reaction. Two epoxy resin boards (200 mm × 45 mm × 0.8 mm) were used to form the reactor walls and acted as dielectric barriers (the dielectric constant $\varepsilon = 3.6$). The high-voltage electrode was made of copper wire, 0.8 mm in diameter. The wire electrode was shaped in a spiral in order to increase the energy density in the reaction volume. The wire-to-wire distance was 10 mm. Two grounded copper net electrodes were fixed on the two sides of the middle epoxy resin board. The total length of the reactor was 200 mm, while the effective length was 150 mm. When no catalyst was used, the gap between the high-voltage electrode and the grounded electrode was 8 mm, resulting in a cross-sectional area for the flow channel of 400 mm^2 and a reaction volume of 60 cm^3. To add a catalyst, it was supported by two pieces of nickel foam (150 mm × 25 mm × 2 mm) fixed to the grounded electrodes. This produced a gap of 6 mm, a cross-sectional area for the flow channel of 300 mm^2 and a reaction volume of 45 cm^3.

2.3. Catalyst

Four kinds of metal oxides, i.e., copper oxide, iron oxide, cobalt oxide, and manganese oxide supported on Al_2O_3/nickel foam (NF), were used as the catalysts with a same mass ratio of 50%:50%:100%. The supported metal oxide (CuO, Fe_3O_4, Co_3O_4, and Mn_2O_3) catalysts were prepared by an incipient wetness impregnation method. The commercial nickel foam support was cut into a definite size (150 mm × 25 mm × 2 mm) and then impregnated with a sol of $(Al_2O_3{\cdot}nH_2O){\cdot}bH_x{\cdot}cH_2O$. After that, it was dried at 393 K for 2 h, and then calcined at 723 K for 4 h. Subsequently, the metal oxides supports were impregnated with aqueous solutions of the corresponding precursors, which included copper nitrate ($Cu(NO_3)_2{\cdot}3H_2O$), iron nitrate ($Fe(NO_3)_3{\cdot}9H_2O$), cobalt nitrate ($Co(NO_3)_2{\cdot}6H_2O$), and manganese nitrate ($Mn(NO_3)_2$). After that, the samples were dried at 393 K for 1 h and calcined at 723 K for 4 h.

2.4. Catalyst characterization

The BET surface area was calculated from the nitrogen adsorption isotherms at 77 K with a surface area analyzer and porisimetry system (SA3100, Beckman Coulter). Prior to the measurements, the samples were evacuated at 343 K for 1 h and then at 423 K for at least 3 h.

XRD data were obtained with the powder method in a Rigaku diffractometer (D/max-IIIA) operated at 30 kV and 30 mA, using Cu Kα radiation. The patterns were recorded over the $10^\circ < 2\theta < 100^\circ$ range and compared to the X-ray powder files to confirm phase identities.

The catalyst microstructure was studied by a Jeol JSM-5910 scanning electron micrographs operating at acceleration voltages 20 kV and equipped with a EDS (Thermo NORAN).

The FT-IR spectra were recorded by using an FT-IR spectrometer (Bruker Tensor 27) at room temperature. Self-supported wafers (15 mm diameter, 15 ± 1 mg) were formed by pressing the catalyst powder scratched from the catalyst. Thirty-two scans were recorded each time.

The toluene removal efficiency, the carbon dioxide selectivity, carbon dioxide and carbon monoxide yields, electric field strength, and specific energy density in the gas phase were defined as follows:

Toluene removal efficiency:

$$\eta_t\ (\%) = \frac{[\text{toluene}]_{\text{inlet}} - [\text{toluene}]_{\text{exhaust}}}{[\text{toluene}]_{\text{inlet}}} \times 100 \quad (1)$$

Carbon dioxide selectivity:

$$S_{CO_2}\ (\%) = \frac{[CO_2]}{[CO] + [CO_2]} \times 100 \quad (2)$$

Carbon dioxide and carbon monoxide yield:

$$CO_x\ (\%) = \frac{[CO] + [CO_2]}{7([C_7H_8]_{\text{before reaction}} - [C_7H_8]_{\text{after reaction}})} \times 100 \quad (3)$$

Electric field strength:

$$E_g\ (\text{kV/cm}) = \frac{V\varepsilon_d}{l_d\varepsilon_g + l_g\varepsilon_d} \quad (4)$$

V is the applied voltage (kV), ε_d is the dielectric constant, l_d is the dielectric thickness, and l_g is the gap distance.

Specific energy density:

$$\text{SED}\ (\text{J/l}) = \frac{\text{discharge power (W)}}{\text{gas flow rate (l/min)}} \times 60 \quad (5)$$

3. Results and discussion

3.1. Toluene removal performance in plasma system under different background gases

3.1.1. Toluene removal efficiency

The experiment was conducted under various background gases, i.e., N_2/Ar and N_2/O_2 with different ratios. The initial concentration of toluene was 50 ppmv and the gas flow rate was 100 ml/min. Fig. 1 shows the dependence of the toluene removal efficiency on electric field strength under N_2/Ar background gas with different ratios. It was found that the toluene removal efficiency increased significantly with the increase of electric field strength and argon content. For example, the toluene removal efficiency of 88.7% was achieved under the electric field strength of 12.2 kV/cm (the applied voltage of 10 kV) with the background gas of nitrogen. However, when argon was used as the background gas, the toluene removal efficiency of 98.1% was observed and at the same time the needed electric field strength was only 4.88 kV/cm (the applied voltage of 4 kV). Adding argon could make the energy density increase also (see Fig. 2). Under the electric field strength of 12.2 kV/cm, the energy density in the reaction was added from 882 J/l (N_2) to 1092 J/l (15%Ar, N_2). The initial discharge voltage under argon is much lower than that under nitrogen. Argon could be ionized easily in DBD then argon plasma comes into being. Generally argon is reckoned as an inertia gas and it is inactive, hence it is used as a protecting gas on many occasions. But for argon plasma, its chemical performance is much different from argon gas, and it could take part in all kinds of chemical reactions. Therefore, adding argon could improve the energy efficiency in the reaction and enhance the toluene removal even under a lower electric field strength.

Fig. 3 shows the effect of oxygen content in the gas stream on toluene removal efficiency for selected applied voltages

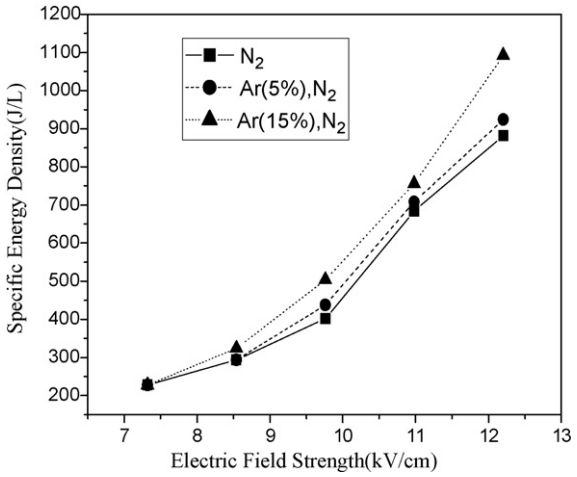

Fig. 2. Dependence of energy density on electric field strength in N_2/Ar background gas: 50 ppmv toluene and 100 ml/min.

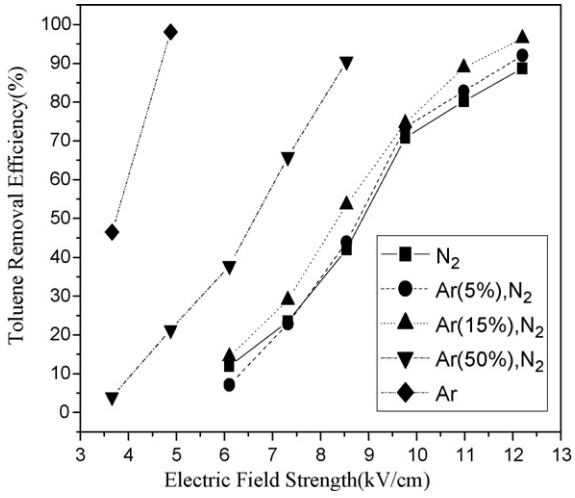

Fig. 1. Dependence of toluene removal efficiency on electric field strength in N_2/Ar background gas: 50 ppmv toluene and 100 ml/min.

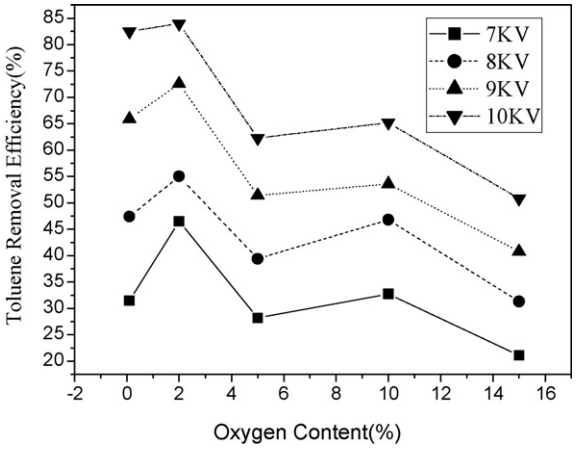

Fig. 3. Dependence of toluene removal efficiency on oxygen content for different applied voltages in N_2/O_2 background gas: 50 ppmv toluene and 100 ml/min.

Table 1
Products and byproducts analysis for toluene decomposition in different background gases

Background gases	Products	Byproducts
N_2, O_2 (>1%)	CO, CO_2 $CO_x = (100 \pm 2)\%$	O_3
N_2, O_2 (<1000 ppm)	CO, CO_2 $CO_x < 65\%$	HCN, CH_4, C_2H_6, $C_{12}H_{26}$
Ar, O_2 (<1000 ppm)	CO, CO_2 $CO_x < 50\%$	$C_{11}H_{24}$, C_9H_{18}, C_3H_6

under N_2/O_2 background gas in the plasma system. The oxygen content includes 0.1, 2, 5, 10, and 15%. The error was under 10%. It was found that toluene-removal efficiency increased with the increase in applied voltage, and the highest toluene-removal efficiency was observed for the gas stream containing 2% oxygen. When the oxygen content was 2% and the applied voltage reached 10 kV, the toluene-removal efficiency of 84% was achieved. When the applied voltage is higher, the produced electric field is stronger and the resumed power is higher. More electrons react with toluene and break the bond between the toluene molecules, thus the removal efficiency of toluene increases. Oxygen plays a very important role in the reaction. Some articles have reported the effect of oxygen content in plasma system [6,7,19,21]. Appropriate oxygen content is essential for toluene destruction.

3.1.2. Products and byproducts analysis

Products and byproducts analysis by GC and GCMS under different background gases in the DBD system is shown in Table 1. When oxygen was enough ($[O_2] \geqq 1\%$), almost all the removed toluene was oxidized to carbon monoxide and carbon dioxide. And ozone was the only byproduct. Whereas when nitrogen and argon were used as background gases (at this time there still existed few oxygen in the gas cylinder), ozone did not exist after reaction, but some other byproducts, such as CH_4, C_2H_6, $C_{12}H_{26}$, and HCN, were detected, and the CO_x yield was smaller than 65% in the N_2 gas stream; $C_{11}H_{24}$, C_9H_{18}, and C_3H_6 were observed as byproducts, and the CO_x yield was lower than 50% in the N_2/Ar and Ar gas.

The relationship between CO_x concentration and electric field strength is shown in Fig. 4. It was found that the concentrations of CO and CO_2 increased with the increase in applied voltage, but the extent for CO_2 increase was more than that of CO. And in the reaction, CO was produced earlier than CO_2. For example, when the electric field strength was lower than 8.5 kV/cm, little CO was produced, and no CO_2 existed in the products. This is because the electron energy is not enough and the oxygen is hard to be ionized in the reaction when the electric field strength is low. Only part of toluene is oxidized to CO, and it is difficult to obtain oxygen and energy and to further oxidize toluene to CO_2. Whereas when the electric field strength is high, CO is oxidized to CO_2, thus the amount of CO_2 increased more than that of CO.

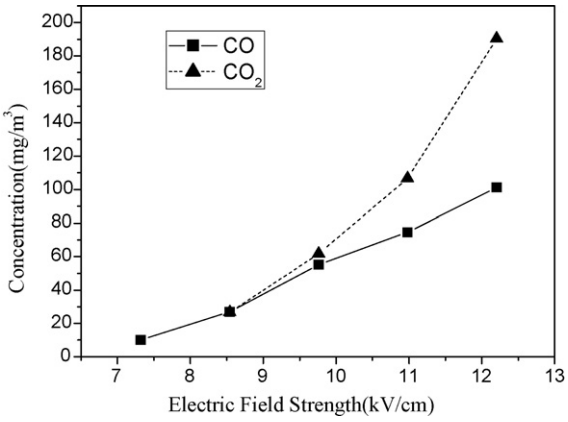

Fig. 4. Dependence of concentrations of CO and CO_2 on electric field strength for different applied voltages in N_2 background gas: 50 ppmv toluene and 100 ml/min.

3.2. Plasma-catalytic performances on toluene decomposition with different catalysts

Fig. 5 shows the effect of catalysts composition on toluene removal efficiency for selected electric field strength (E_d) in the DBD–catalyst system. The reaction condition of 5%O_2/N_2 and 500 ml/min was applied to the system. The initial toluene concentration was 50 ppmv. It was found that the toluene removal efficiency (η_t) with metal oxides loaded on the support was much higher than that with no metal oxides loaded (only NF). And the sequence on toluene removal for different active metal oxide components in the catalysts was Mn > Cu > Fe > Co. When the applied voltage was 11 kV and the electric field strength was 17.5 kV/cm, the toluene-removal efficiency was 83.16% for plasma-manganese oxide catalyst system.

Fig. 6 shows the dependence of carbon dioxide selectivity on electric field strength for different catalysts. From this figure, it was found that the S_{CO_2} ranged from 60 to 80% in the DBD reactor with various active components in the catalysts and the S_{CO_2} for manganese oxide catalyst was more than 75% and it was higher than that for others. With no active component, the S_{CO_2} was only 61%, while 70% for Fe and Cu catalysts and 63% for Co catalysts. The selectivity was enhanced with active components due to the toluene oxidation near and/or on the catalyst surface.

The influence of the catalyst on ozone formation is presented in Fig. 7. It shows that ozone concentration increased with the

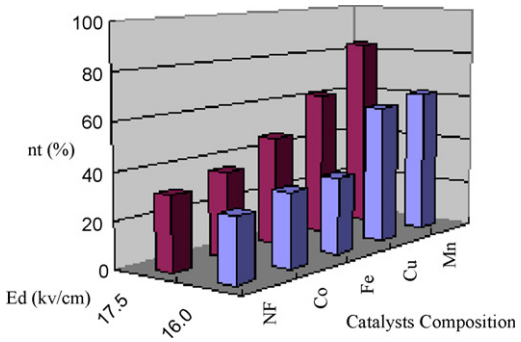

Fig. 5. Dependence of toluene removal efficiency on electric field strength for different catalysts: 50 ppmv toluene, 5% O_2, and 500 ml/min.

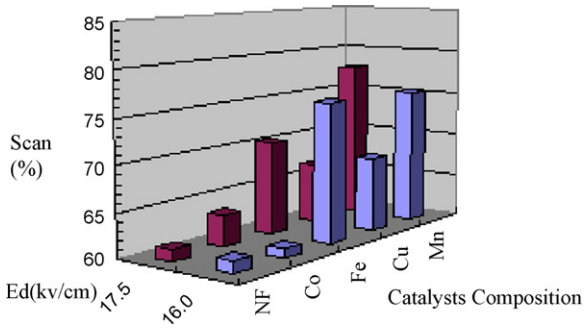

Fig. 6. Dependence of carbon dioxide selectivity on electric field strength for different catalysts: 50 ppmv toluene, 5% O_2, and 500 ml/min.

increase in electric field strength and the manganese oxide catalyst could restrain the production of ozone to a great extent. With the electric field strength of 16 and 17.5 kV/cm, the respective ozone concentration of 3.6 and 6.0 mg/m^3 was achieved. For the cobalt oxide catalyst, the ozone concentration was 34.6 mg/m^3 (16 kV/cm) and 36.6 mg/m^3 (17.5 kV/cm) which was lower than that of more than 40 mg/m^3 for other metal oxides and only NF catalysts. Ozone as the main long-living radical was transported to the catalyst and could take part in heterogeneous oxidation reactions on its surface.

Futamura et al. reported the plausible mechanism for MnO_2-catalyzed decomposition of O_3 as following reactions. This reaction belongs to the secondary Rideal–Eley type reaction, that is, the oxygen atoms are formed on the surface of MnO_2 (O^*) and a part of desorbed $O^*\leftarrow$ is present as $O(^3P)$ in the gaseous phase, then benzene reacts with O^* and creates the oxide products [12].

$$O_3 + {}^* \rightarrow O_2 + O^* \quad (1)$$

$$O_3 + O^* \rightarrow O_2 + O_2{}^* \quad (2)$$

$$C_6H_6 + O^* \rightarrow \text{Products} \quad (3)$$

3.3. Reaction mechanism and dynamics analysis

As the former article reported that decomposition of toluene via DBD could generally be achieved through three channels, i.e., (1) electron impact dissociation, (2) gas-phase radical reactions, and (3) ion–molecule reactions [19]. The major pathway leading to toluene removal in N_2 or Ar plasma is through electron impact dissociation since toluene does not directly react with nitrogen molecules.

$$C_6H_5CH_3 + e \rightarrow C_6H_4CH_3 + H + e \quad (4)$$

$$\rightarrow C_6H_4 + CH_3 + e \quad (5)$$

Another possible mechanism for toluene removal pertains to ion reactions. In plasmas, ions are produced simultaneously along with the generation of electrons based on charge balance. The electron–ion pairs are produced through electron-impact ionization processes. In this case, N_2 or Ar impacts with electron and the excited nitrogen or argon species comes into being. Such excited species react with toluene, resulting in the benzene ring broken and some radicals like CH_3 and H are produced. Then the broken benzene ring links with the radicals, thus some steady products, for example, $C_{12}H_{26}$, $C_{11}H_{24}$, and C_9H_{18}, form. Nitrogen atoms should be reckoned as a source in the formation of HCN. The possible reaction process by non-thermal plasma is indicated as follows:

$$e + N_2 \rightarrow e + N_2(A) \quad (6)$$

$$e + N_2 \rightarrow N^* + N + e(N^*\text{iselectronicallyexcitednitrogenspecies}) \quad (7)$$

$$e + Ar \rightarrow e + Ar^* + e(Ar^*\text{iselectronicallyexcitedargonspecies}) \quad (8)$$

$$C_6H_5CH_3 + N^*, Ar^* \rightarrow C_6H_5{}^\bullet + CH_3{}^\bullet + H^\bullet \quad (9)$$

$$CH_3{}^\bullet + H^\bullet \rightarrow CH_4 \quad (10)$$

$$CH_3{}^\bullet + CH_3{}^\bullet \rightarrow C_2H_6 \quad (11)$$

$$C_6H_5{}^\bullet + CH_3{}^\bullet + H^\bullet \rightarrow C_{12}H_{26}, C_{11}H_{24}, C_9H_{18} \quad (12)$$

On the other hand, in the presence of N_2/O_2, the main radicals in the plasma reaction are $OH^\bullet$, $O(^1D)$, $O(^3P)$, O_3, and N; however, O and O_3 reactions are negligible [22,23]. And the rate (electron impact):rate (ions):rate (OH radical attack) equals to 10^4:1:10 [6]. Hydrocarbons oxidize by such radicals, then CO and CO_2 form.

$$C_6H_5CH_3 + O^+, O_2{}^+, N, N_2{}^+ \rightarrow C_6H_5CH_3{}^+ + O, O_3, N, N_2 \quad (13)$$

$$C_6H_5CH_3{}^+ + e \rightarrow C_6H_5 + CH_3 \quad (14)$$

$$C_6H_5CH_3 + OH \rightarrow C_6H_5CH_3OH \quad (15)$$

$$\rightarrow C_6H_5CH_2 + H_2O \quad (16)$$

$$C_6H_5CH_3 + O \rightarrow C_6H_5CH_2O + H \quad (17)$$

$$C_6H_5CH_3 + O_3 \rightarrow C_6H_5CHO_2 + H_2O \quad (18)$$

Reactions (19)–(22) are the major reactions leading to toluene conversion with the catalyst under N_2/O_2 gases. M

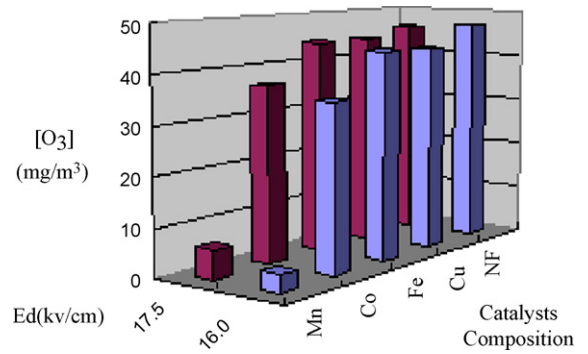

Fig. 7. Dependence of ozone concentration on electric field strength for different catalysts: 50 ppmv toluene, 5% O_2, and 500 ml/min.

indicates the catalyst metal atom. As shown in reactions (19) and (20), the first step of the catalytic conversion with the metal oxide catalyst involves the toluene adsorption on the O atom, that is, the active site of the catalyst. The O atom on the catalyst would attack the C atom of the adsorbed toluene to form the intermediates and break C_6H_5–CH_3 bond. Thereafter, the O atom of another metal oxide adjacent to the intermediate attacks the C of the intermediate, breaking the C–H bond in the benzene ring, and CO, CO_2, and H_2O are intermediately formed on O. This step is the surface reaction. Then CO and CO_2 are desorbed from the metal oxide catalyst. Reactions (21) and (22) describe another catalytic conversion of the CH_3 radical that is produced by the first step of reaction (19).

$$C_6H_5CH_3 + MO \rightarrow C_6H_5{-}MO + CH_3 \quad (19)$$

$$C_6H_5{-}MO + O \rightarrow CO + CO_2 + H_2O + MO \quad (20)$$

$$CH_3 + MO \rightarrow CH_2{-}MO + H \quad (21)$$

$$CH_2{-}MO + O \rightarrow CO + CO_2 + H_2O + MO \quad (22)$$

The kinetics equation is denoted as

$$-\frac{dC}{dt} = k[e][C] \quad (23)$$

The electrons concentration is a constant under the identical electric field and air pressure. Eq. (6) is simplified as

$$-\frac{dC}{dt} = k_s[C] \quad (24)$$

Integrate from the inlet ($C = [C_0]$, $t = 0$) to the outlet,

$$-\ln\frac{C}{C_0} = k_s t \quad (25)$$

Combing Eq. (1) and rearranging,

$$-\ln(1-\eta) = k_s t \quad (26)$$

The rate constant of DBD reactor as a function of electric field combined with/without catalyst under different background gas can be denoted as reactions (27)–(30) in the form of Arrhenius equation. This fact demonstrates that plasma reaction under argon gas and plasma combined with catalysis can remarkably enhance activities for toluene oxidation.

$$K = 1.18e^{-36.1/E} \quad (N_2,\ \text{plasma system}) \quad (27)$$

$$K = 28.01e^{-27.03/E} \quad (\text{Ar},\ \text{plasma system}) \quad (28)$$

$$K = 0.33e^{-30.77/E} \quad (5\%O_2, N_2,\ \text{plasma system}) \quad (29)$$

$$K = 170.21e^{-114.34/E} \quad (5\%O_2, N_2,\ \text{plasma-manganese oxide catalyst system}) \quad (30)$$

3.4. Characterization of the catalysts

The characterization of the catalysts was compared before/after discharge by BET, XRD, SEM, FT-IR, and EDS. The catalyst was carried out after about 40 h experiments of toluene decomposition with plasma application. The electric field strength was controlled at 17.5 kV/cm, the gas streams contained 50 ppmv toluene, the oxygen content was 5%, and the gas flow rate was 500 ml/min.

Table 2
Comparison of BET surface area of the catalysts

Active components of catalysts	The net weight of the sample (g)	BET surface area (m^2/g)
Co	0.1938	6.035
Cu	0.2102	10.699
Fe	0.1937	24.324
Mn	0.2117	35.192

3.4.1. BET surface area

The results of BET are listed in Table 2. It could be seen that the metal oxide catalysts sequence of BET surface area is Mn > Fe > Cu > Co. Manganese oxide owns a much larger BET surface area. Commonly speaking, a higher BET surface area means a higher dispersion of the catalyst and a bigger contact area between active component and gas, which leads to a better catalytic activity. Therefore, the catalytic activity of manganese oxide catalyst is best, and this is in good consistent with the results of the plasma-catalytic performances test on toluene decomposition.

3.4.2. XRD spectra

The XRD spectra of the four kinds of catalysts before and after reaction are presented in Fig. 8(a)–(d). The results of the catalysts are shown in Table 3. By matching with JCPDS file data, it is indicated from the observed peaks that Ni metal was clearly observed in every catalyst and it comes from the catalytic carrier, i.e., nickel foam. Aluminates such as $CuAl_2O_4$, $FeAl_2O_4$, $CoAl_2O_4$, and $MnAl_2O_4$ with cubic structure are formed after calcining. The four different catalysts have their own corresponding metal oxides. From Figs. 4 and 5, it is found that the aluminates for Cu and Fe decompose to the

Table 3
The XRD results of catalysts

Catalyst	Before reaction	After reaction
$CuO/Al_2O_3/NF$	Ni (cubic) $CuAlO_2$ (hexagonal) $CuAl_2O_4$ (cubic) CuO (monoclinic)	Ni (cubic) CuO (monoclinic)
$Fe_2O_3/Al_2O_3/NF$	Ni (cubic) $FeAl_2O_4$ (cubic) Fe_2O_3 (cubic) γ-Fe_2O_3 (tetragonal)	Ni (cubic) γ-Fe_2O_3 (tetragonal)
$Co_3O_4/Al_2O_3/NF$	Ni (cubic) $CoAl_2O_4$ (cubic) Co_2AlO_4 (cubic) Co_3O_4 (cubic)	Ni (cubic) Co_2AlO_4 (cubic) Co_3O_4 (cubic)
$Mn_2O_3/Al_2O_3/NF$	Ni (cubic) Mn_2O_3 (orthorhombic) $MnAl_2O_4$ (cubic)	Ni (cubic) Mn_3O_4 (cubic) $MnAl_2O_4$ (cubic)

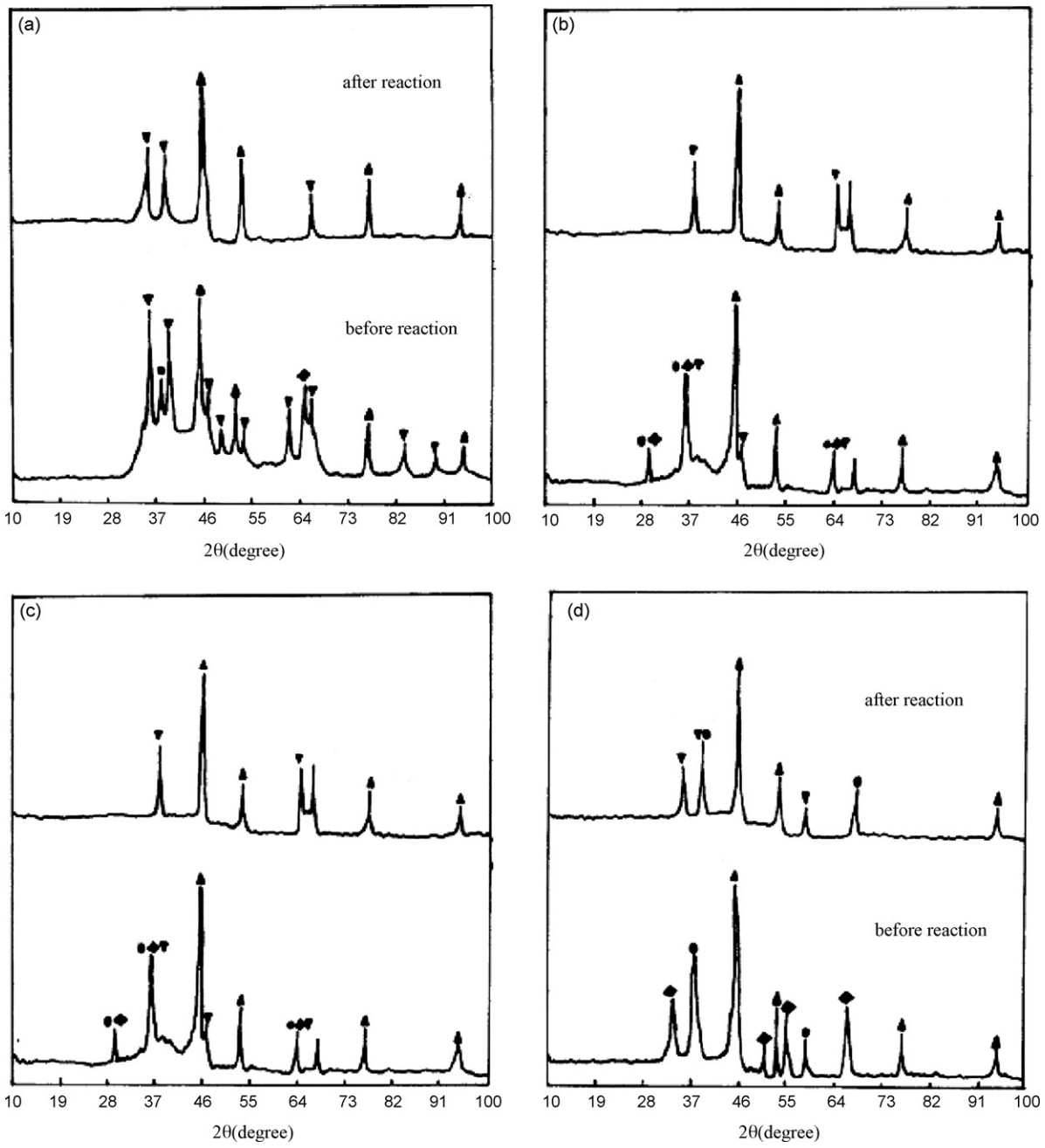

Fig. 8. (a) XRD results of CuO/Al_2O_3/NF catalyst: (▲) Ni; (●) $CuAlO_2$; (◆) $CuAl_2O_4$; (▼) CuO. (b) XRD results of Fe_2O_3/Al_2O_3/NF catalyst: (▲) Ni; (●) $FeAl_2O_4$; (◆) Fe_2O_3; (▼) γ-Fe_2O_3. (c) XRD results of Co_3O_4/Al_2O_3/NF catalyst: (▲) Ni; (●) $CoAl_2O_4$; (◆) Co_2AlO_4; (▼) Co_3O_4. (d) XRD results of Mn_2O_3/Al_2O_3/NF catalyst: (▲) Ni; (●) $MnAl_2O_4$; (◆) Mn_2O_3; (▼) Mn_3O_4.

corresponding oxides in the plasma process. In addition, in Fig. 7, the composition of Mn_2O_3 in the catalyst changes to Mn_3O_4 after discharge. And the proportion of manganese oxide increases, while the aluminate decreases after DBD application. The oxidation capability of Mn_3O_4 is better than that of Mn_2O_3, as a result, it is in favor of enhancing the toluene oxidation.

3.4.3. SEM image

Fig. 9(A) shows the SEM images of the metal oxide support—nickel foam (magnification values of 85× and 1000×). This figure illustrates that nickel foam has a pentagonal framework, and on the surface of the foam nickel there have a lot of small holes which lead to a large surface area. Fig. 9(B)–(E) compare the SEM images of the four kinds of catalysts before and after reaction (magnification values of 1000×). It is found that the active components of the catalysts are loaded on the foam nickel with crystal form widespread over the support surface. The catalytic components disperse on the foam nickel support in different kinds of crystallite, such as block state, piece state, grain, and powder. In the cobalt oxide catalyst with block structure before reaction, the local accumulation is serious and some smaller particles disperse

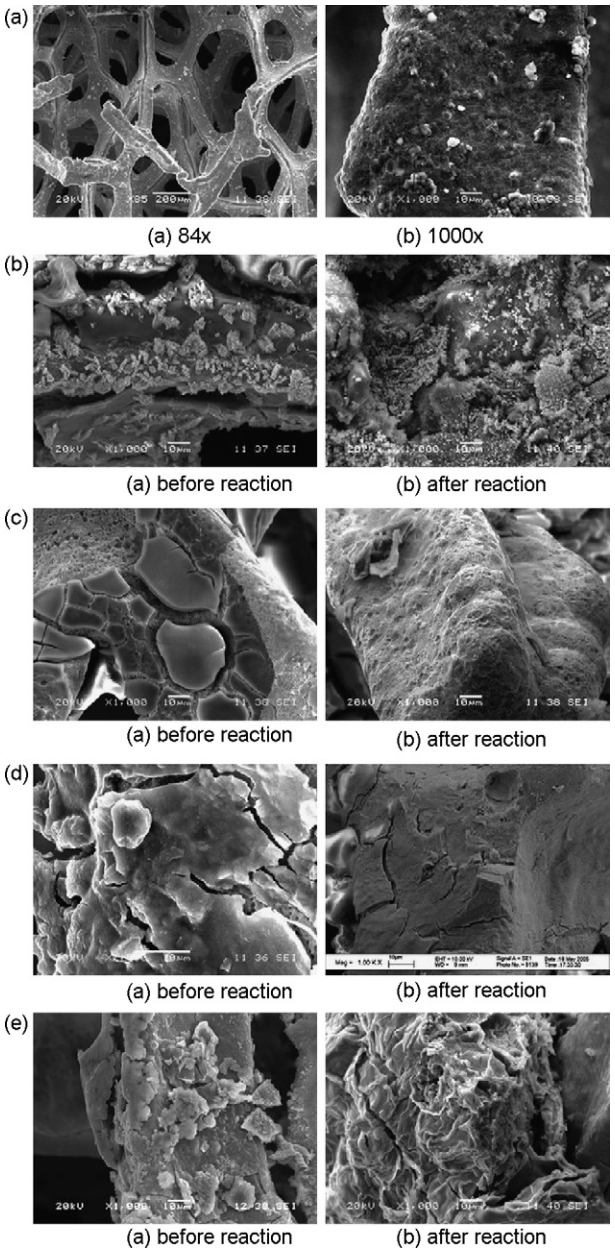

Fig. 9. (A) SEM micrographs of nickel foam: (a) 85× and (b) 1000×. (B) SEM micrographs of CuO/Al_2O_3/NF catalyst (1000×): (a) before reaction and (b) after reaction. (C) SEM micrographs of Fe_2O_3/Al_2O_3/NF catalyst (1000×): (a) before reaction and (b) after reaction. (D) SEM micrographs of Co_3O_4/Al_2O_3/NF catalyst (1000×): (a) before reaction and (b) after reaction. (E) SEM micrographs of Mn_2O_3/Al_2O_3/NF catalyst (1000×): (a) before reaction and (b) after reaction.

on the smooth surface of the catalyst crystal. After reaction, the surface is also covered with block state on the NF framework. The crystal structure for iron oxide catalyst is mainly smooth piece state and grain, and the local accumulation before reaction is less than cobalt oxide catalyst. In addition, there is seldom local accumulation after reaction and the surface is rough and porous. The crystal structure of manganese oxide catalyst is piece state, but the dispersion is better than iron oxide catalyst. The crystal surface is rough and some particulates exist. After reaction, the crystal shape changes and a lot of gauffers come into being. The crystal structure of copper oxide catalyst is mainly grain and there are a few local accumulations before reaction. Whereas after reaction, the granularity of the grain on the catalyst surface becomes smaller, the distribution becomes more uniform, and the dispersion is higher.

The ultrafine particle catalysts have large specific surface and less-perfect crystal lattice with a large number of vacancies, which induce a high catalytic activity. It indicates that plasma enhances the dispersion of the active species, increases the stability as well as the activity of the catalysts, and strengthens the oxidation capability of the catalyst, therefore removal of toluene is promoted. It was reported that some unusual chemical activities had been achieved when plasma species were involved in the catalyst surface reactions, which led to efforts to apply plasmas directly to prepare more effective catalysts [24,25]. Zhang et al. demonstrated that the glow discharge treatment leads to a higher and stable dispersion of active species over the support. Also a better activity and a significantly enhanced stability of the catalysts were achieved [26]. Chen et al. found that the conversion and selectivity of the catalysts prepared by glow discharge plasma were superior to those obtained from the conventional catalysts [27]. The results of this reaction were in good agreement with those given in these articles.

3.4.4. FT-IR spectra

The FT-IR spectra of catalysts before and after reaction are presented in Fig. 10(a)–(d). Except the absorption bands of the adsorbed water between 3000 and 3600 cm^{-1}, 1600 and 1670 cm^{-1}, and the band of CO_2 at 2349 cm^{-1} in the spectra, the band of aluminate at about 750 cm^{-1} is detected in the spectra of the catalyst before reaction. The bands at 500–610 cm^{-1} correspond to the vibration of the metal oxide (Co–O, Mn–O, Fe–O, and Mn–O). The spectra of the catalyst after reaction are quite the same with those before reaction, but the transmittivity increases, which suggests that the grain of the catalyst becomes smaller and highly dispersed on the support. Especially, the band of aluminate in the spectrum of the catalyst disappears after reaction, while the band of metal oxide is sharper. It suggests that the aluminate decomposes to the corresponding oxide under the electric field. These results are consistent with those of the XRD and SEM. In addition, the bands at 1380 cm^{-1} which represent the characteristic peak of methyl are detected in all the catalysts, it therefore suggests that some organic compounds deposit or adsorb on the surface of the catalyst.

3.4.5. EDS spectrum

The results of EDS suggest that the element of C is found on the catalysts after reaction, which means that some organic compounds are deposited on the catalysts after plasma reaction. It is because ozone produced in the plasma reaction is dissociated to O_2 and $O(^3P)$ on the surface of the catalyst, then $O(^3P)$ reacts with toluene and organic compounds are created. This is in accord with the results of FT-IR.

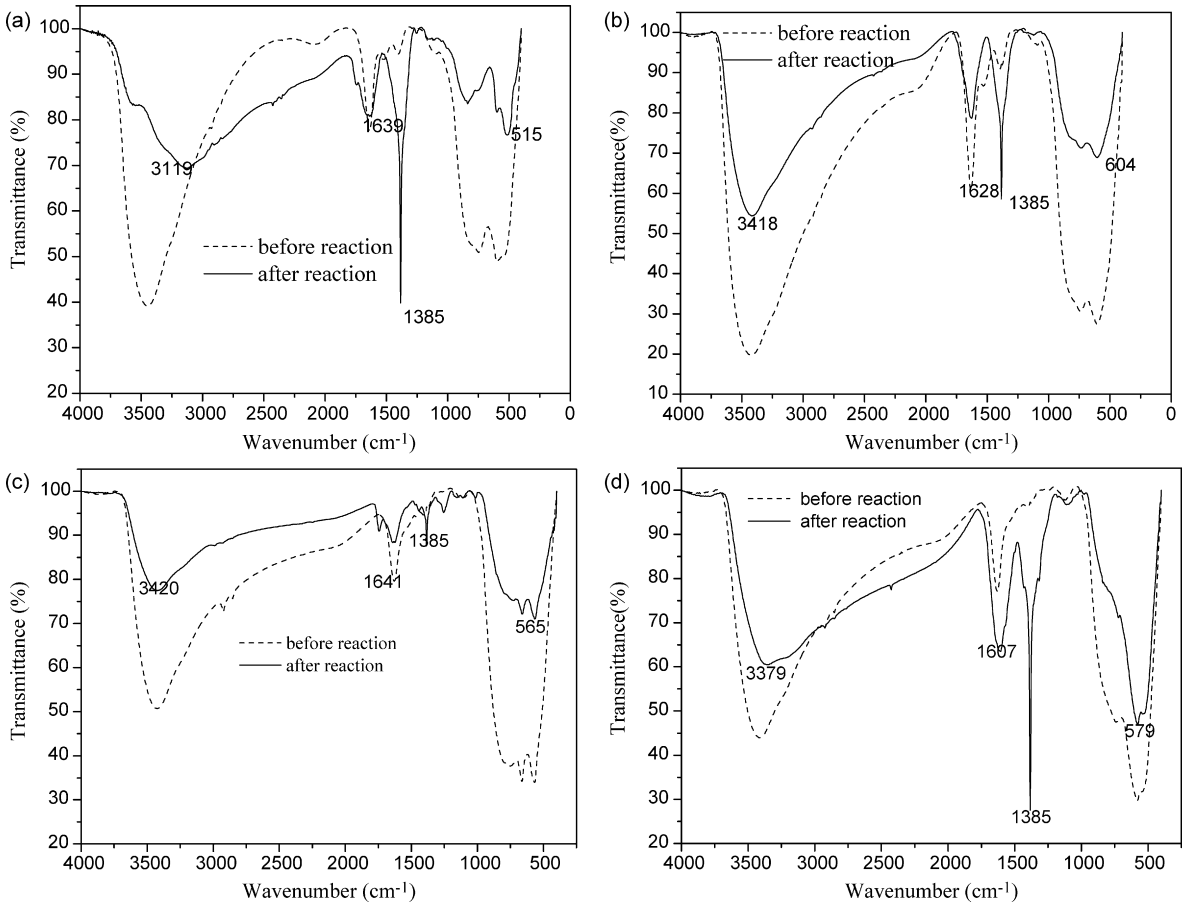

Fig. 10. (a) FT-IR spectra of CuO/Al_2O_3/NF catalyst before and after reaction. (b) FT-IR spectra of Fe_2O_3/Al_2O_3/NF catalyst before and after reaction. (c) FT-IR spectra of Co_3O_4/Al_2O_3/NF catalyst before and after reaction. (d) FT-IR spectra of Mn_2O_3/Al_2O_3/NF catalyst before and after reaction.

4. Conclusions

Toluene removal performance in plasma system under different background gases has great discrepancy. Adding argon could improve the energy efficiency and enhance the toluene removal greatly. The combination of dielectric barrier discharge and metal oxide catalyst could improve the toluene-removal efficiency and carbon dioxide selectivity, and suppress byproduct (such as ozone) formation. Manganese oxide/alumina/NF was demonstrated as the most effective catalyst for toluene removal. The potential reaction mechanism and dynamics were analyzed. In addition, a catalytic mechanism in the combined plasma with catalyst system was proposed that the DBD could enhance the dispersion of the active species, increase the stability, as well as the activity of the catalyst, strengthen the oxidation capability of the catalyst, consequently the removal of toluene could be promoted.

Acknowledgment

This work was partially supported by National Nature Science Foundation of China (20577011), Guangdong Province Key Scientific and Technological Project (2001367, 2002254), and Guangzhou City Key Scientific and Technological Project (2001-Z-016-01).

References

[1] M. Okubo, T. Kuroki, H. Kametaka, T. Yamamoto, IEEE Trans. Ind. Appl. 2 (2000) 868.
[2] S.J. Yu, M.B. Chang, Plasma Chem. Plasma Process 21 (2001) 311.
[3] S. Futamura, T. Yamamoto, P.A. Lawless, IEEE Trans. Ind. Appl. 2 (1995) 1453.
[4] A.A. Khassin, B.L. Pietruszka, M. Heintze, V.N. Parmon, React. Kinet. Catal. Lett. 82 (2004) 131.
[5] R. Rudolph, K.-P. Francke, H. Miessner, Plasma Chem. Plasma Process 22 (2002) 401.
[6] H.M. Lee, M.B. Chang, Plasma Chem. Plasma Process 23 (2003) 541.
[7] H.R. Snyder, G.K. Anderson, IEEE Trans. Plasma Sci. 26 (1998) 1695.
[8] M.P. Cal, M. Schluep, Environ. Prog. 20 (2001) 151.
[9] U. Roland, F. Holzer, F.-D. Kopinke, Catal. Today 73 (2002) 315.
[10] A. Ogata, N. Shintani, K. Mizuno, S. Kushiyama, in: Proceedings of the IEEE Industry Application Society Annual Meeting, Decomposition of Benzene Using Non-thermal Plasma Reactor Packed with Ferro-electric Pellet, New Orleans, Louisiana, 5–9 October 1997, pp. 1975–1982.
[11] C. Ayrault, J. Barrault, N. Blin-Simiand, F. Jorand, S. Pasquiers, A. Rousseau, J.M. Tatibouët, Catal. Today 89 (2004) 75.
[12] S. Futamura, H. Einaga, H. Kabashima, L.Y. Hwan, Catal. Today 89 (2004) 89.
[13] Z. Mingqian, Z. Bing, T.C. Karl, Appl. Catal. B Environ. 13 (1997) 123.
[14] C.S. Jeffrey, T.Y. Chang, Catal. Today 44 (1998) 11.
[15] S.C. Kim, J. Hazard. Mater. B 91 (2002) 285.
[16] K.M. Parida, S. Amarendra, Appl. Catal. A Gen. 182 (1999) 249.

[17] P. Papaefthimiou, T. Ioannides, X.E. Verykios, Appl. Catal. B Environ. 13 (1997) 175.
[18] M.M.R. Peijen-Jeurissen, J.J. Jorna, B.E. Nieuwenhuys, G. Sinquin, C. Petit, J.P. Hindermann, Catal. Today 54 (1999) 65.
[19] Y.-F. Guo, D.-Q. Ye, K.F. Chen, J.-C. He, W.L. Chen, J. Mol. Catal. A Chem. 245 (2006) 93.
[20] Y.-F. Guo, D.-Q. Ye, K.F. Chen, Y.-F. Tian, Plasma Chem. Plasma Process 26 (2006) 237.
[21] H.M. Lee, M.B. Chang, Plasma Chem. Plasma Process 21 (2001) 329.
[22] K. Urashima, J.-S. Chang, IEEE Trans. Dielectrics Electric. Insulat. 7 (2000) 602.
[23] H. Kohno, A.A. Berezin, J.-S. Chang, M. Tamura, T. Yamamoto, A. Shibuya, S. Honda, IEEE Trans. Ind. Appl. 34 (1998) 953.
[24] C.-J. Liu, G.P. Vissokov, Ben W.-L. Jang, Catal. Today 72 (2002) 173.
[25] M.B. Kizling, S.G. Järås, Appl. Catal. A Gen. 147 (1996) 1.
[26] Y.-P. Zhang, P.-S. Ma, X.-L. Zhu, C.-J. Liu, Y.-T. Shen, Catal. Commun. 5 (2004) 35.
[27] M.H. Chen, W. Chu, X.Y. Dai, X.W. Zhang, Catal. Today 89 (2004) 201.